Shahrood University of Technology

Journal of Mining and Environment (JME)

Journal homepage: www.jme.shahroodut.ac.ir

Iranian Society of Mining Engineering (IRSME)

# Investigation of the Swelling Pressure of Marlstone in the Vicinity of Cations

Amirreza Kavandi and Ramin Doostmohammadi*

*Mining Engineering Department, Faculty of Engineering, University of Zanjan, Zanjan, Iran*

***Article Info***

*Received 31 January 2025*

*Received in Revised form 28 August 2025*

*Accepted 20 September 2025*

*Published online 20 September 2025*

*DOI: 10.22044/jme.2025.15669.3010*

***Keywords***

*Swelling control*

*Cation retention capability*

*Na+ cation*

*Ca2+ cation*

***Abstract***

So far, limited research has been conducted on the swelling behavior of Marlstone in the presence of cations. In this study, swelling pressure experiments were performed on rock samples obtained from the Marash Dam, located in northwest Iran. The specimens underwent wetting and drying cycles to achieve an equilibrium condition before cation infiltration. Rock specimens were infiltrated with distilled water and with 1, 2, and 3 mol/L solutions of sodium chloride (NaCl) and calcium chloride (CaCl2). The findings suggest that as the concentration of the solutions rises, the swelling pressure of Marlstone diminishes. Furthermore, at the same concentrations, the swelling pressure of samples soaked in CaCl2 solutions was less than that of those treated with NaCl solutions. Additionally, Marlstone saturated with Ca2+ ions exhibited greater resistance to leaching compared to those saturated with Na+ ions. The findings of this research can be applied to control the swelling pressure of weak rocks in proximity to support systems.

## 1. Introduction

Rock swelling, a time-dependent phenomenon following excavation, poses significant challenges in rock mechanics. Marlstone, primarily composed of 35% to 56% clay and 65% to 35% carbonate, exhibits water absorption and swelling behavior. Its soft and weak nature upon contact with water categorizes it as a "problematic rock." Consequently, in water-related projects such as dam construction, marlstone is viewed as a troublesome swellable rock that can cause considerable damage. One method to mitigate this swelling is through the infiltration of cations The complex nanoscale interactions governing cation efficacy can be elucidated through advanced computational modeling. For instance, a recent coarse-grained molecular dynamics study by Tong et al. [1] simulated the wetting of montmorillonite clay aggregates, establishing a direct micro-macro relationship between swelling stress and the distribution of clay tactoids (stacked layers). Their findings demonstrate that swelling stress is intrinsically dependent on the total number of tactoids, following a well-defined logarithmic relationship. This underscores that any mitigation strategy, such as cation infiltration, must ultimately alter the microscopic fabric and tactoid distribution to effectively control macroscopic swelling pressure. The efficacy of cation infiltration is governed by complex nanoscale interactions within clay minerals. Insights from Molecular Dynamics simulations, utilizing the Clay force field and software such as LAMMPS, reveal that cation behavior is complicated, with their valency, hydration energy, and ionic radius critically influencing the structure of interlayer water and the resultant swelling processes [2]. While divalent cations like calcium ($Ca^{2+}$) possess higher hydration energy and can create a more organized hydration shell within the clay interlayer at the nanoscale compared to monovalent sodium ($Na^{+}$), their macroscopic effect is the opposite. The strong electrostatic

Corresponding author: ramin.doostmohammadi@znu.ac.ir (R. Doostmohammadi)

bridges formed by $Ca^{2+}$ ions between negatively charged clay platelets act as powerful constraints, effectively suppressing overall volumetric swelling and resulting in significantly lower swelling pressure. In contrast, $Na^{+}$ ions form weaker diffuse layers, allowing for easier separation of clay particles and greater macroscopic expansion. Consequently, from an engineering perspective, the infiltration of $Ca^{2+}$ cations is a highly effective strategy for mitigating the swelling pressure of clay-rich rocks like marlstone. Recent studies have examined the swelling behavior of clays in response to the infiltration of salt solutions. Various laboratory experiments have investigated the chemical impacts of cations on the swelling ability of different bentonites, revealing that a decrease in solution salinity correlates with increased swelling behavior [3-18]. As pore water salinity increases, the thickness of the double layer diminishes, resulting in reduced swelling pressure [11]. Wakim et al. [19] explored the impact of solution chemistry on the swelling and shrinkage of Tournemire shale, demonstrating a significant reduction in swelling pressure with increasing solution concentration. Zhu et al. [20] and Ye et al. [21] investigated how salt solutions impact the swelling characteristics of compacted GaoMiaoZi (GMZ) bentonite in China, showing that the salinity of the infiltrating solutions significantly influences both swelling pressure and swelling strain, with an increase in the concentration of these solutions leading to a reduction in both parameters. Additionally, Chen et al. [22] studied the swelling pressure of bentonite subjected to cyclic infiltrations of distilled water and various concentrations of NaCl solutions (0.1M, 1M, and 2M), noting that salinization and desalinization processes yielded markedly different effects on swelling behavior, even at identical concentrations. Chen et al. [23] observed that high concentrations of NaCl solutions significantly reduce the swelling strain of GMZ bentonite and further investigated the combined effects of vertical dead load and NaCl solution on swelling behavior, concluding that the influence of the NaCl solution diminishes with increasing vertical dead load. Zhang et al. [24] developed an empirical formula to estimate the maximum swelling strain of GMZ bentonite based on vertical stress and salt concentration. Liu et al. [25] explored how hyperalkaline solutions influence the swelling pressure of GMZ bentonite, concentrating on the impacts of $Na^{+}$ cations and $OH^{-}$ anions. Their results showed that higher levels of $Na^{+}$ cations hinder crystalline and double-layer swelling, whereas greater amounts of $OH^{-}$ anions enhance double-layer swelling and lead to rearrangement of the fabric. In this study, swelling pressure experiments were carried out on Marlstone samples from the Marash Dam, using distilled water, calcium chloride ($CaCl_2$), and sodium chloride (NaCl) solutions at varying concentrations. The outcomes were analyzed to assess how cations and their concentrations affect the swelling pressure of the Marlstone samples. This paper aims to propose a solution for controlling the swelling behavior of weak rocks in hydraulic engineering projects (e.g., dam construction and water-related structures) through cation injection. Furthermore, it investigates the long-term stability of this swelling reduction method when exposed to cyclic water exposure in aquatic environments. This study introduces two key innovations: Firstly, a novel sample stabilization protocol was developed, wherein all rock specimens undergo systematic wetting-drying cycles before cation exposure to establish a stable swelling baseline. This preconditioning methodology effectively eliminates variability arising from heterogeneous mineral distribution and fracture history, thereby enabling accurate comparison of cation effects. Secondly, an experimental framework was established to comprehensively evaluate leaching resistance under simulated hydraulic conditions. The implemented system rigorously evaluates the long-term stability of cation-treated specimens under simulated hydraulic conditions. This analysis provides critical data for developing strategies to mitigate swelling pressure in hydraulic infrastructure.

## 2. Materials and Methods

### 2.1. Materials

The mineralogical composition of the mudstone was analyzed using X-ray diffraction (XRD) with a Bruker AXS diffractometer (Table 1). A representative portion of the air-dried marlstone sample was finely ground using an agate mortar and pestle. The powdered sample was sieved to obtain the −200 mesh fraction, which was then loaded into the diffractometer's specimen holder and compacted with a glass slide. The prepared sample was scanned at a rate of 1.2°/min over a 2θ range; with diffraction patterns recorded using a strip-chart recorder. Mineral identification was performed by comparing characteristic peaks with reference standards from

the Powder Diffraction File. For specimen infiltration, distilled water, $CaCl_2$, and NaCl, solutions were employed. To prepare calcium chloride ($CaCl_2$) and sodium chloride (NaCl) solutions with the required molarity, the appropriate masses of dehydrate salt (Merck, Germany) were calculated based on the desired concentration. The weighed salts were dissolved in 80% of the final volume of distilled water at 22±1°C under continuous stirring to ensure complete dissolution. The solutions were then adjusted to their final volumes in calibrated volumetric flasks to achieve precise molarity. The molarity was verified using titration measurements. The exceptionally low mechanical strength of the Marlstone resulted in frequent specimen fracturing during machining operations. Despite extensive preparation efforts, only two intact samples could be successfully obtained. To address this sample size limitation, the experimental protocol was augmented through: (1) testing multiple fluid concentration gradients (4 varying solution concentrations), and (2) implementing repeated wetting-leaching cycles (5 washing processes for each specimen), and (3) using swelling equations and models in describing phenomena. This methodological adjustment reliably characterized trends in swelling behavior, including both increasing and decreasing patterns, without compromising measurement accuracy.

## 2.2. Test apparatus

The experimental apparatus for the swelling pressure test, developed at the University of Zanjan, is illustrated in Figure 2. This setup includes a rigid frame (1), screw-driven plunger (2), gearbox (3), load cell (4), specimen ring (5), two porous stones (6), a steel ball (7) for load transmission, a stainless steel piston for load distribution (8), a specimen container for solution infiltration (9), and a high-precision mechanical gauge (10) for measuring displacement, along with a pressure monitor (data logger) (11) (see Figure 2a).


**Figure 1. Location of the Marash Dam in northwest Iran.**

**Table 1. Mineralogical properties of Marlstone specimens.**

| Specimen No. | Montmorillonite (%) | Illite (%) | Kaolinite (%) | Chlorite (%) | Quartz (%) | Feldspar (%) | Calcite (%) | Vermiculite (%) |
|---|---|---|---|---|---|---|---|---|
| M.S.1 | 11 | 23 | 12 | 4 | 8 | 37 | 4 | 1 |
| M.S.2 | 4 | 10 | 5 | 0 | 61 | 0 | 20 | 0 |

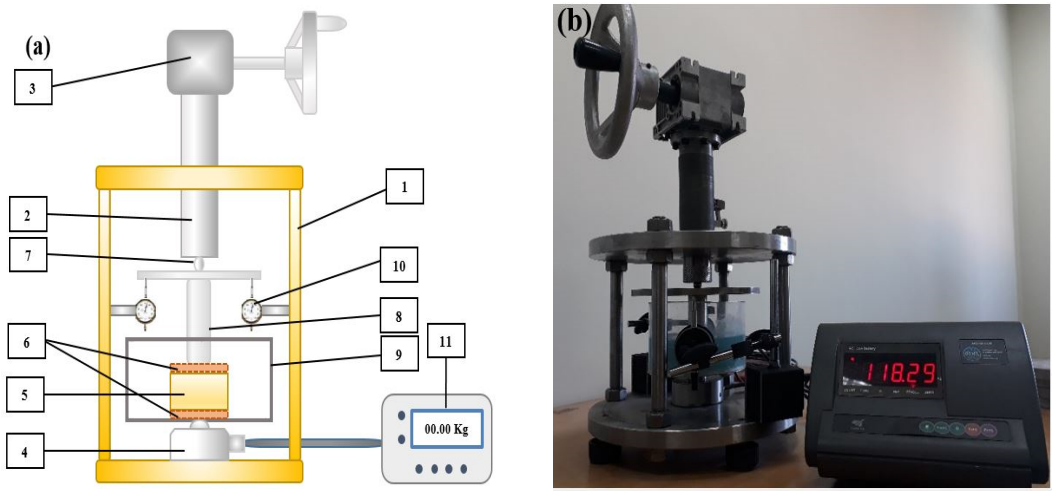


**(a) schematic of test apparatus** **(b) picture of test apparatus**

**Figure 2. Setup for swelling pressure test**

### 2.3. Specimen Preparation

Cylindrical rock specimens of Marlstone, measuring 50 mm in diameter and 20 mm in height, were arranged. The specimens were machined using a high-precision lathe, ensuring no visible cracks or structural alterations. Distilled water and six solutions (1M, 2M, and 3M $CaCl_2$, and 1M, 2M, and 3M NaCl) were utilized for specimen saturation.

### 2.4. Test Procedure

Following specimen preparation, each rock specimen was placed inside a cylindrical enclosing ring to prevent lateral deformation, with porous plates installed above and below the specimen. The ring made of stainless steel that holds the rock sample was subsequently put together with the other parts of the testing equipment. Given the variability of mineralogical properties within the rock block, the swelling behavior of different specimens cannot be directly compared; therefore, it is essential to use unique specimens within the vicinity of solutions in cycles. Furthermore, cyclic infiltration of a single specimen leads to varying swelling pressures during initial periods [26-29]. To address this issue, specimens underwent wetting and drying cycles in a custom apparatus to achieve a steady swelling pressure before cation infiltration (see Figure 3). The swelling pressure of the rock, as illustrated in Figure 3, rises with the increase in the number of cycles. Specimens M.S.1 and M.S.2 achieved steady pressure by the 9th (Figure 3a) and 7th (Figure 3b) cycles, respectively.

Table 1 shows that sample M.S.1 has higher montmorillonite content than sample M.S.2, which corresponds to its greater swelling pressure, as also evidenced in Figure 3.

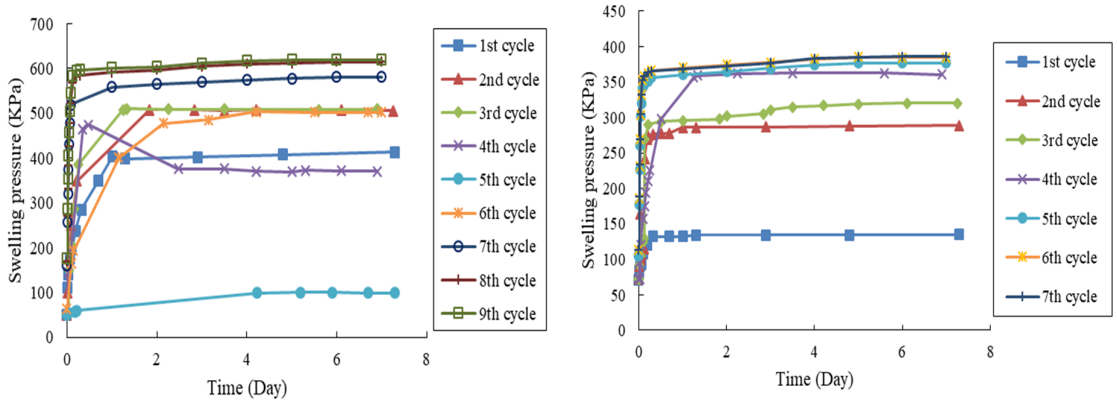


**(a) M.S.1** **(b) M.S.2**

**Figure 3. Cyclic infiltration of Marlstones with distilled water**

Following completion of the wetting-drying cycles, each specimen was infiltrated with 400 mL of test solutions, including distilled water (control), calcium chloride ($CaCl_2$), and sodium chloride (NaCl) at specified concentrations. Following each infiltration cycle, specimens were saturated with distilled water to eliminate the influence of preceding cations and return them to their initial state. Subsequently, swelling pressure was measured under constant-volume conditions at a temperature of 22±1°C.

## 3. Results

Swelling pressure tests were conducted on two rock specimens (M.S.1 and M.S.2) with infiltrations of $CaCl_2$ and NaCl solutions at varying concentrations (1, 2, and 3 mol/L) and distilled water. The evolution of swelling pressures for the two specimens is presented in Figure 4. The maximum swelling pressures for M.S.1 and M.S.2 were measured at 618.95 kPa and 385.81 kPa, respectively. For the infiltration of $CaCl_2$ and NaCl solutions at different concentrations, the swelling pressure of M.S.1 decreased from 576.65 kPa (1M NaCl) to 273.36 kPa (3M NaCl) (Figure 4a) and from 536.42 kPa (1M $CaCl_2$) to 156.8 kPa (3M $CaCl_2$) (Figure 4b). Similarly, the swelling pressure of M.S.2 decreased from 310 kPa (1M NaCl) to 147 kPa (3M NaCl) (Figure 4c) and from 285.23 kPa (1M $CaCl_2$) to 63.44 kPa (3M $CaCl_2$) (Figure 4d). This trend suggests that as the concentration of infiltrating solutions rises, the swelling pressure of Marlstone diminishes. Compared to the swelling pressure measured with distilled water, the

swelling pressure observed with salt solution infiltration was significantly reduced, indicating that the presence of salt solutions significantly reduces the swelling pressure of Marlstone. This finding is consistent with the results reported by Castellanos et al. [11] regarding compacted FEBEX bentonite and by Ye et al. [21] concerning compacted GMZ bentonite.

Figure 5 illustrates the percentage reduction in swelling pressure of Marlstone specimens. The reduction in swelling pressure under $Na^+$ infiltration was lower than that under $Ca^{2+}$ cations at the same solution concentration, suggesting a greater controlling effect of $Ca^{2+}$ on swelling pressure compared to $Na^+$.

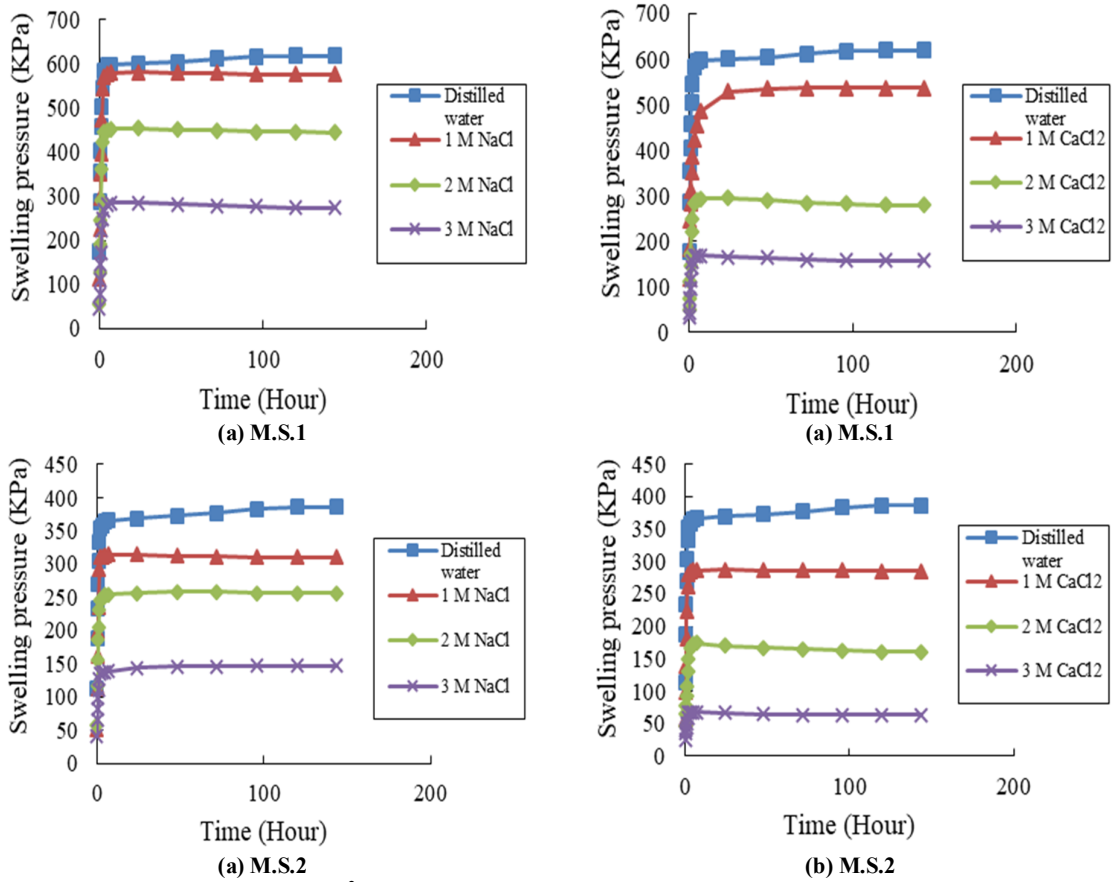


**Figure 4. Effect of $Na^+$ and $Ca^{2+}$ cations on swelling pressure of Marlstone under different salt solutions.**

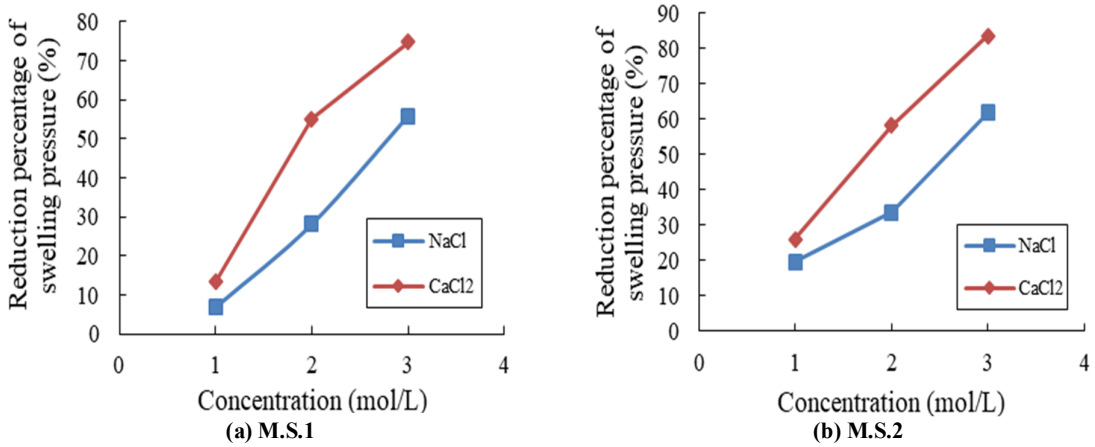


**Figure 5. Reduction percentage of swelling pressure of Marlstone under different salt solutions**

### 3.1. Prediction of The Maximum Swelling Pressure

The swell-time curves exhibited a hyperbolic pattern, which can be approximated using Equation (1) [30]. By rewriting the equation and plotting t/p (time/swell pressure) versus t at different time intervals, it can be linearized. This linear relationship is then used to calculate parameters a and b. This procedure was used to analyze the swelling behavior of all samples across 14 distinct conditions, each with a different concentration of cation-containing solutions. The results are presented in Figure 6 and Tables 2-3.

The maximum value of swelling pressure, Pmax (KPa), can be calculated using Equation (2):

$$P = \frac{t}{a + bt} \tag{1}$$

$$P_{max} = \lim_{t\to\infty} P(t) = \lim_{t\to\infty}\left(\frac{1}{\left(\frac{a}{t}\right) + b}\right) = \frac{1}{b} \tag{2}$$

Where are:

t- the elapsed time (Hour),

P- the swelling pressure (KPa),

Pmax- the maximum swell pressure (KPa),

a and b- coefficients to be fixed.

This value (1/b), which is predicted by Equation 2 using the parameter b derived earlier, represents the theoretical maximum swelling potential. To validate this predictive capability, the calculated values were plotted against experimentally measured values, as shown in Figure 7. The resulting plot demonstrates a strong agreement between predicted and observed values, as evidenced by data points clustering closely around the 1:1 bisector and a correlation coefficient exceeding 0.9. This high degree of correspondence validates the predictive power of Equation 1 for characterizing the swelling behavior.

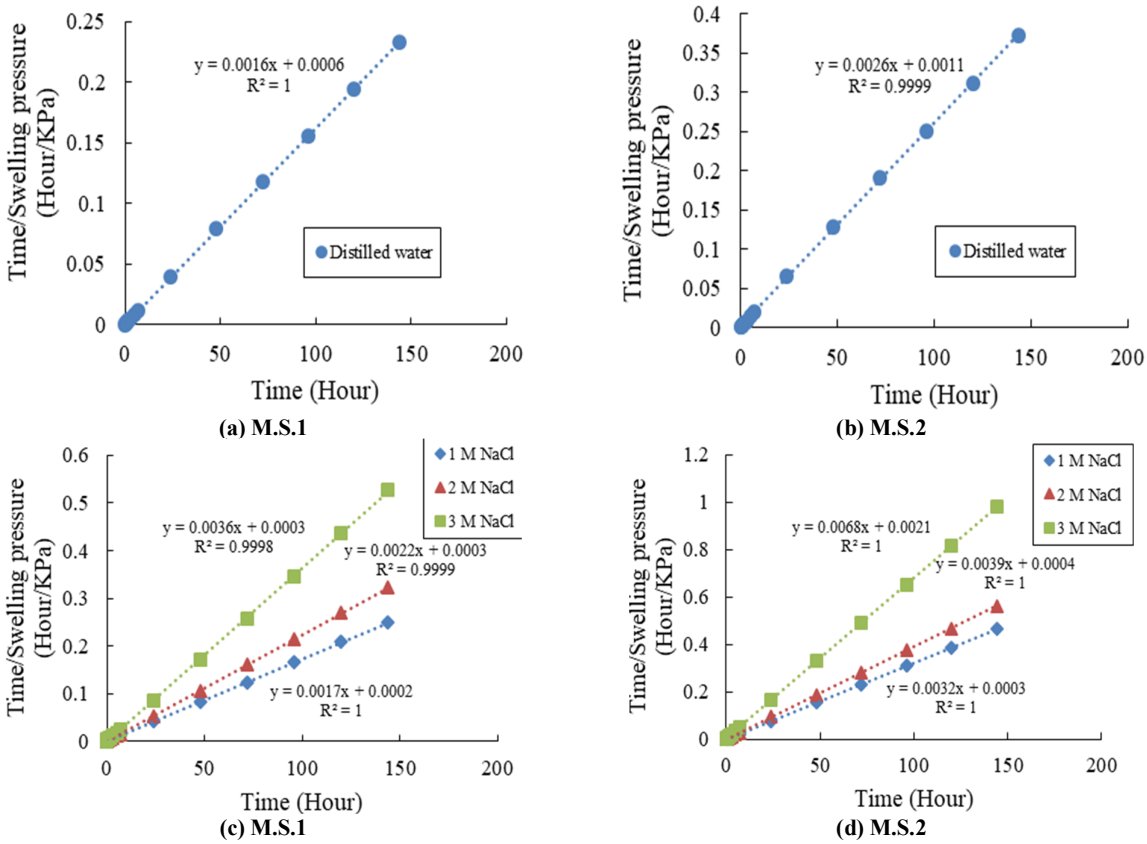


(a) M.S.1 (b) M.S.2

(c) M.S.1 (d) M.S.2

**Figure 6. (Time/Swelling pressure) vs. time relationship under different salt solutions**

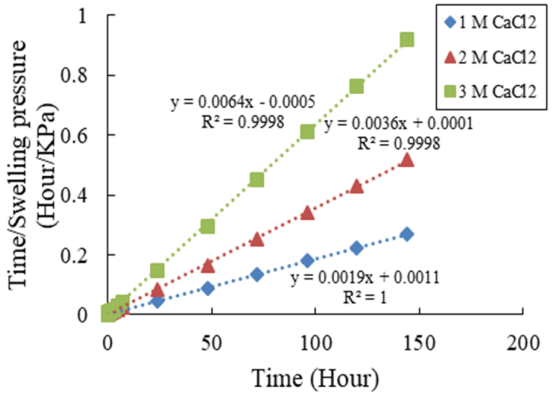


(e) M.S.1

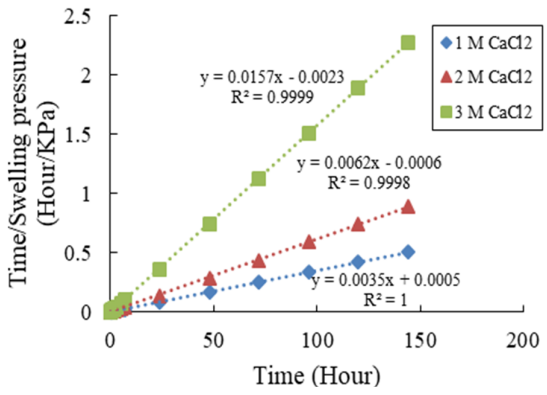


(f) M.S.2

**Continuous of Figure 6. (Time/Swelling pressure) vs. time relationship under different salt solutions**

**Table 2. Prediction of maximum swelling pressure ($P_{max}$) for all tests (M.S.1)**

| Solutions | Relationship | a | b | Correlation coefficient | $P_{max}$ (Kpa) |
|---|---|---|---|---|---|
| Distilled water | $y = 0.0016x + 0.0006$ | 0.0006 | 0.0016 | 1 | 625 |
| 1 M NaCl | $y = 0.0017x + 0.0002$ | 0.0002 | 0.0017 | 1 | 588.23 |
| 2 M NaCl | $y = 0.0022x + 0.0003$ | 0.0003 | 0.0022 | 0.999 | 454.54 |
| 3 M NaCl | $y = 0.0036x + 0.0003$ | 0.0003 | 0.0036 | 0.999 | 277.77 |
| 1 M $CaCl_2$ | $y = 0.0019x + 0.0011$ | 0.0011 | 0.0019 | 1 | 526.31 |
| 2 M $CaCl_2$ | $y = 0.0036x + 0.0001$ | 0.0001 | 0.0036 | 0.999 | 277.77 |
| 3 M $CaCl_2$ | $y = 0.0064x - 0.0005$ | -0.0005 | 0.0064 | 0.999 | 156.25 |

**Table 3. Prediction of maximum swelling pressure (Pmax) for all tests (M.S.2)**

| Solutions | Relationship | a | b | Correlation coefficient | $P_{max}$ (Kpa) |
|---|---|---|---|---|---|
| Distilled water | $y = 0.0026x + 0.0011$ | 0.0011 | 0.0026 | 0.999 | 384.61 |
| 1 M NaCl | $y = 0.0032x + 0.0003$ | 0.0003 | 0.0032 | 1 | 312.5 |
| 2 M NaCl | $y = 0.0039x + 0.0004$ | 0.0004 | 0.0039 | 1 | 256.41 |
| 3 M NaCl | $y = 0.0068x + 0.0021$ | 0.0021 | 0.0068 | 1 | 147.05 |
| 1 M $CaCl_2$ | $y = 0.0035x + 0.0005$ | 0.0005 | 0.0035 | 1 | 285.71 |
| 2 M $CaCl_2$ | $y = 0.0062x - 0.0006$ | -0.0006 | 0.0062 | 0.999 | 161.29 |
| 3 M $CaCl_2$ | $y = 0.0157x - 0.0023$ | -0.0023 | 0.0157 | 0.999 | 63.69 |

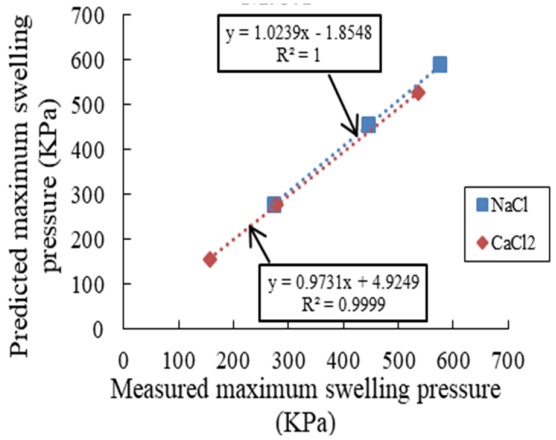


(a) M.S.1

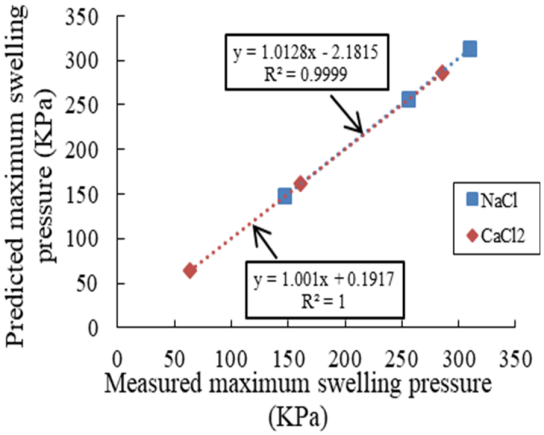


(b) M.S.2

**Figure 7. Predicted swell vs. measured ones for infiltrating with CaCl2 solutions and NaCl.**

## 4. Discussion

The swelling of clay minerals primarily occurs through two mechanisms: crystalline swelling and double-layer swelling. Crystalline swelling begins with the adsorption of water molecules onto the surfaces of clay particles or through the hydration of exchangeable cations such as $K^+$, $Na^+$, $Ca^{2+}$,

and $Mg^{2+}$ located between the 2:1 clay layers. These clays are composed of an aluminum octahedral sheet situated between two silica tetrahedral sheets (TOT) [31-34]. This process is characterized as short-term swelling due to its rapid occurrence. Once the majority of hydrates have been adsorbed, the rate of surface hydration diminishes, leading to the onset of the diffuse double-layer (DDL) swelling mechanism [35]. Diffuse double-layer swelling, a long-term process, occurs over an extended timeframe [21].

When Marlstone specimens come into contact with distilled water, the exchangeable interlayer cations absorb the water and become hydrated. This process leads to the disintegration of thick crystals into thinner structures. The new thinner structures fill the larger voids between the coarse particles without changing the distance between their layers [5]. Consequently, the aggregates expanded (step 1 in Figure 8) and the specimen swelled (crystalline swelling). Following the completion of crystalline swelling, primary swelling ceased, and the dispersal of the diffuse double layer initiated the secondary swelling stage (step 2 in Figure 8).

During the swelling process, multiple diffuse double layers formed in the pores between the crystalline and interlayer spaces. As the diffuse double layer dispersed, quasi-crystals gradually separated into separate layers and occupied the inter-aggregate space, leading to continued aggregate swelling (step 2 in Figure 8). Eventually, all quasi-crystals were subdivided into individual layers (step 3 in Figure 8), at which point double layer swelling was complete and the swelling pressure of the specimen reached an equilibrium condition. Thus, the secondary phase of swelling predominantly occurs through the dispersion of the diffuse double layer.

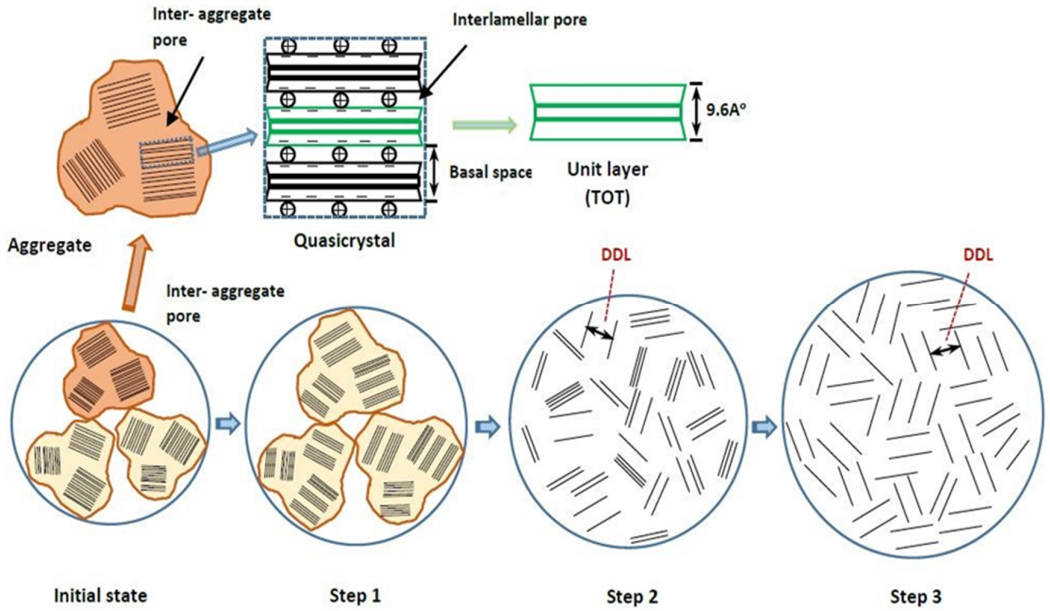


**Figure 8. Schematic diagram of a swelling process of clay [7, 36].**

The DLVO theory (Derjaguin-Landau-Verwey-Overbeek) is a classical framework for explaining the behavior of colloids and clay particles in aqueous environments. This theory considers two primary Electrostatic repulsive and Van der Waals attractive forces. In this model, the balance between these two forces determines the swelling behavior of clays. However, the DLVO theory alone cannot fully account for the differences in clay behavior when exposed to different cations (e.g., $Na^+$ vs. $Ca^{2+}$). Supplementary Boltzmann Distribution of Counter-ions equation can be used to describe this limitation. The concentration of counter-ions ($C_{ic}$) in the interlayer water is given by Equation (3) [37]:

$$C_{ic} = D.C_{ib}.exp\left(-\frac{zq\psi_c}{kT}\right) \quad (3)$$

where:

z - Valence of the counter-ion (1 for $Na^+$, 2 for $Ca^{2+}$).

D- Thickness of the interfacial water layer (m).

Cib- Bulk concentration of counterions ($mol/m^3$).

q- Elementary charge ($1.602 \times 10^{-19}$ C).

ψc- Electric potential at the counterion plane (V).

K- Boltzmann constant ($1.381 \times 10^{-23}$ J/K).

T-- Absolute temperature (K).

Due to the lower valence (z = 1) of monovalent ions (e.g., $Na^+$), the exponential term ($\exp\left(-\frac{zq\psi_c}{kT}\right)$) is larger, resulting in higher counter-ion concentrations in the interlayer. This enhances the electrostatic repulsion between clay platelets, resulting in increased swelling.

In divalent ions (e.g., $Ca^{2+}$) with (z = 2), the exponential term is smaller, reducing interlayer counter-ion concentrations. Consequently, electrostatic repulsion weakens, promoting the formation of compact tactoid structures, leading to lower swelling.

The electrostatic Gibbs energy ($G_e$) of interaction between clay platelets depends on the charge density of the substitutional cations (σ) and the counter-ions ($\sigma_c$) in the interlayer water, as described by Equation (4) [37]:

$$\sigma_c = 2.F.Z.D.C_{ib}.\mathrm{Sinh}\left(\frac{Z.q.\psi_c}{K.T}\right) \quad (4)$$

Where:

$\sigma_c$- Charge density of counter-ions in the interlayer water (C/m²).

F- Faraday constant, representing the charge per mole of electrons.

At high solution concentrations, σc exceeds the platelet charge density (σ), promoting tactoid stability and reduced swelling. At low concentrations, σc<σ, leading to stronger repulsion and increased swelling.

In the use of monovalent cations ($Na^+$), A lower z reduces $\sigma_c$. when $\sigma_c < \sigma$, the net electrostatic interaction becomes repulsive, leading to increased swelling.

In the use of Divalent cations ($Ca^{2+}$), A higher z increases $\sigma_c$ . when $\sigma_c > \sigma$, the net electrostatic interaction becomes attractive, leading to decreased swelling.

Osmotic swelling occurs within the diffuse double layer of negatively charged clay surfaces and is constrained by the Debye–Huckel length, also known as the electrostatic screening length ($k^{-1}$). The quantity of cations and water in the diffuse double layer determines its thickness ($k^{-1}$) and the resultant swelling and shrinkage status of clay as depicted in Figure9 [38].

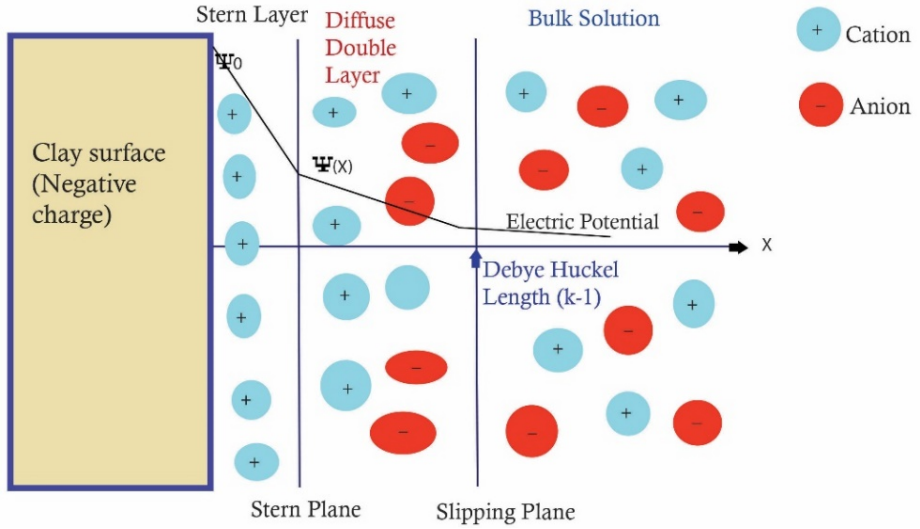


**Figure 9. Debye-Huckel length within the diffuse double layer [38].**

The presence of cations in the diffuse double layer reduces $k^{-1}$, shields negative surface charge of interacting particles, and promotes particles attraction and stability. Therefore, the swelling behavior of swellable rocks is fundamentally governed by the thickness of the diffuse double layer (DDL), quantified by $k^{-1}$ [38]:

$$K^{-1} = \sqrt{\frac{\epsilon_r.\epsilon_0.K_B.T}{2.N_A.e^2.I}} \quad (5)$$

$$I = \frac{1}{2}\sum_i m_i.{z_i}^2 \quad (6)$$

Where:

$\varepsilon_r$- Dielectric constant of water

$\varepsilon_0$- Permittivity of free space ($C^2/J{\cdot}m$)

$K_B$- Boltzmann constant (J/K)

T- Absolute temperature (K)

$N_A$- Avogadro's number ($6.02\times10^{23}$ $mol^{-1}$)

e- Elementary charge (C)

I- Ionic strength = (mol/L)

$m_i$- molality of ion (mol.l-1)

The ionic strength term (I) introduces a critical distinction between $Na^+$ and $Ca^{2+}$. The equation demonstrates that the utilization of divalent ions leads to an increase in the ionic strength, consequently resulting in a reduction of the double layer thickness.This analysis quantitatively demonstrates that calcium cations outperform sodium cations.

According to Figure 5 and Table 4, infiltration of 1, 2, and 3 mol/L NaCl solutions resulted in a swelling pressure decrease of 6.83%, 28.08%, and 55.83% for M.S.1, and 19.65%, 33.55%, and 61.89% for M.S.2 compared to distilled water. Similarly, infiltration of 1, 2, and 3 mol/L $CaCl_2$ solutions led to a swelling pressure decrease of 13.33%, 55%, and 74.66% for M.S.1, and 26.07%, 58.29%, and 83.55% for M.S.2 compared to distilled water. These results indicate that the percentage reduction in swelling pressure of Marlstone specimens increases with higher concentrations of infiltrating solutions.

**Table 4. Percentage reduction in swelling pressure of Marlstone samples under different salt solutions**

| Concentration (mol/L) | Na Cl (M.S.1) | CaCl2(M.S.1) | Na Cl (M.S.1) | CaCl2(M.S.1) |
|---|---|---|---|---|
| **1** | 6.83% | 13.33% | 19.65% | 26.07% |
| **2** | 28.08% | 55.00% | 33.55% | 58.29% |
| **3** | 55.83% | 74.66% | 61.89% | 83.55% |

The experiments conducted on Marlstone show that using saline solutions reduces the swelling pressure, and this is directly related to a decrease in the thickness of the DDL layer. The result observed in laboratory experiments aligns with the theory that relates the thickness of the DDL layer to the inverse square of the concentration [20, 39]. Consequently, higher solution concentrations result in decreased DDL thickness and, therefore, diminished repulsive forces between clay particles [38, 39]. As a result, materials experience reduced swelling [5, 11, 40].

It is well established that the hydration forces associated with $Na^+$ and $Ca^{2+}$ cations are distinct. Montmorillonite that utilizes $Na^+$ as the exchangeable cation is capable of producing a thickness that corresponds to three or four layers of monomolecular water on its surface, whereas montmorillonite with $Ca^{2+}$ yields only two layers of water monomolecular [35, 41]. This suggests that Marlstone with $Na^+$ has a larger basal space compared to that with $Ca^{2+}$, leading to more significant swelling in Marlstone infiltrated with $Na^+$ cations. At comparable concentrations, the swelling pressure of Marlstone treated with $CaCl_2$ solutions is less than that of Marlstone treated with NaCl solutions (Figure 10). This observation suggests that the influence of $Ca^{2+}$ on swelling pressure reduction is more significant than that of $Na^+$.

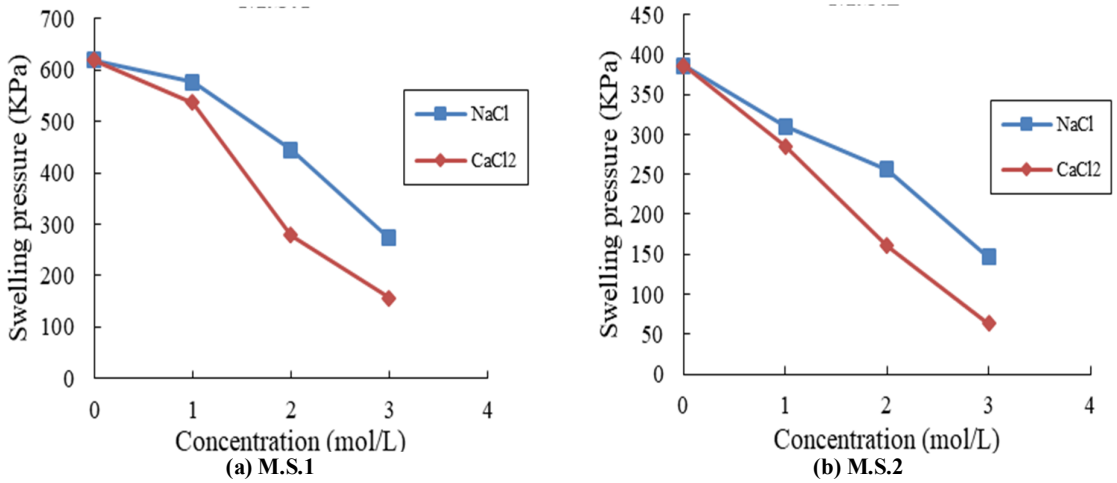


**(a) M.S.1** **(b) M.S.2**

**Figure 10. Comparison of cation type's effect on swelling pressure of Marlstone**

When NaCl infiltrates clay, montmorillonite undergoes sodium-melting, forming bonding molecules. Due to the low valence capacity of $Na^+$, the bond is weak and $Na^+$ can be readily separated. Conversely, infiltration of $CaCl_2$ results in a strong bond between $Ca^{2+}$ and water molecules due to the higher valence of $Ca^{2+}$, leading to stabilization and hardening of the interlamellar pore space [20]. In this study, after the infiltration of 2 M NaCl, the specimens were washed with distilled water for one cycle to return to their initial state (Figure 11a and Figure 11b). However, specimens infiltrated with 2 M $CaCl_2$ did not reach their initial swelling pressure even after five cycles (Figure 11c and Figure 11d). This suggests that Marlstone saturated with $Ca^{2+}$ cations exhibits greater resistance to leaching compared to $Na^+$ cations, indicating that $Ca^{2+}$ cation serves as a more stable swelling control agent in comparison to $Na^+$.

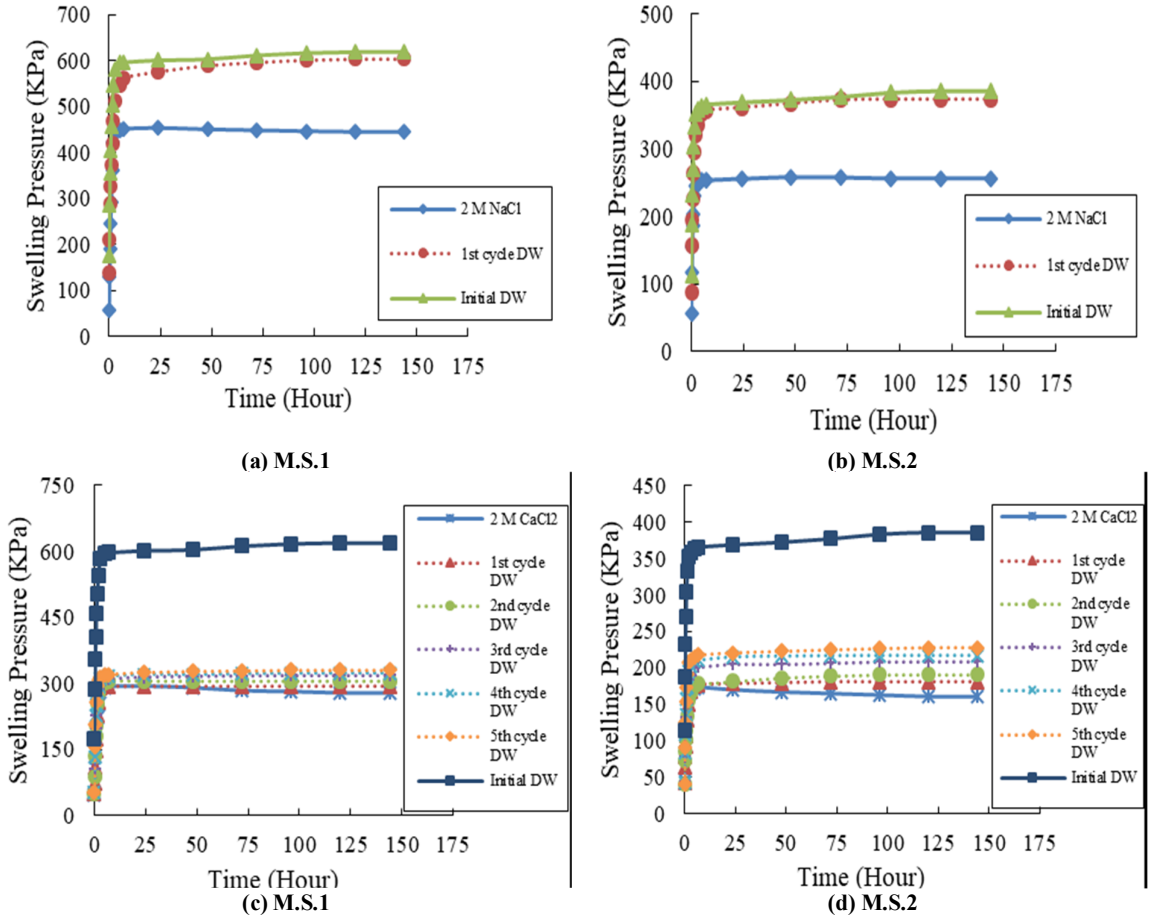


**Figure 11. The resistance of infiltrated Malstone against washing with distilled water (DW: Distilled water).**

## 5. Practical Implications

One of the practical implications of this research is the use of cations to mitigate swelling behavior in projects where swellable rock is present alongside support systems such as concrete linings. These rocks can exert significant pressure on support structures, potentially causing damage. A relevant example is the powerhouse cavern of the Masjed-Soleyman hydropower plant, where the concrete lining is adjacent to swelling mudstone and subjected to swelling pressure. Pressure cells installed near the lining have recorded the swelling behavior of the rock over time (Figure12) [42].

Annually, following the onset of the rainy season and after a specific time lag, water infiltrates the mudstone layers. This infiltration leads to increased swelling compared to previous cycles. This rise in swelling pressure has been recorded at three different monitoring stations (Figure 13). Although the laboratory tests conducted in this study were not performed on the mudstone from the Masjed-Soleyman hydropower plant, the results indicate that calcium cation injection can significantly reduce swelling pressure in similar projects facing swelling-related issues.

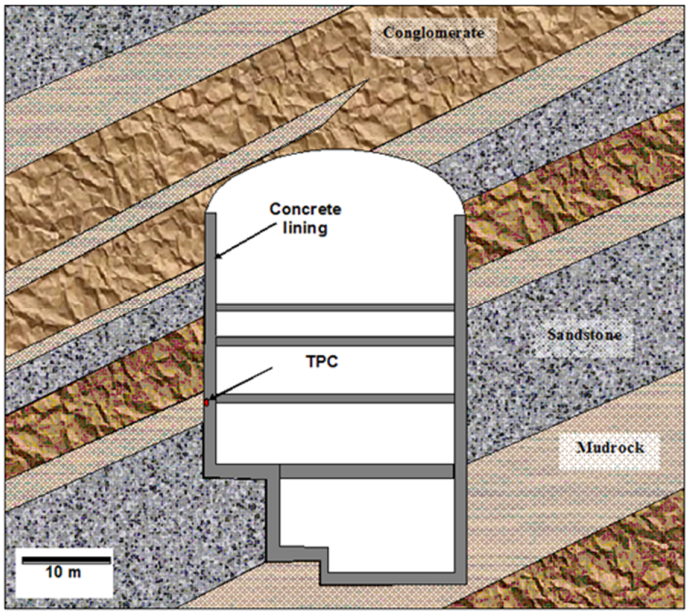


**Figure 12. Powerhouse and contacted mudstone layer [42].**

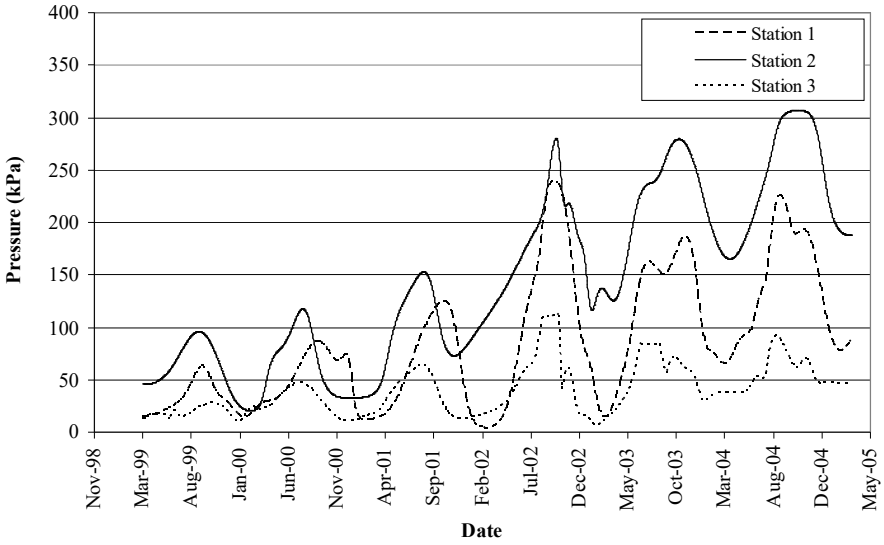


**Figure 13. The monitoring results of Total Pressure Cells in different positions [42].**

Additionally, Figure 12 shows that in the last year for which data were available, the recorded pressure varied from 90 to 320 kPa between different stations. This suggests that due to the heterogeneity of the rock mass and the varying content of swelling minerals, swelling pressure differs across locations, leading to varying responses to the injection of different types and concentrations of cations. Therefore, it is recommended that, in such cases, specialized laboratory tests (similar to those proposed in this study) be conducted to determine the optimal treatment approach.

The amount of stress induced in the concrete lining by the swelling force depends on the location of the swellable layer and the shape of the lining. In the present case (Figure 12), the lining is a vertical wall fixed at both ends by anchors and horizontal concrete slabs, consequently behaving as a cantilever beam. The modulus of rupture applied on the other side of the neutral line of this beam, which is located directly opposite the swelling layer, is obtained using Equation 7.

$$\sigma_t = \frac{P.L}{b.t^2} \quad (7)$$

where:

$\sigma_t$- Modulus of rupture

P- Swelling force

L- Lining length

b- Liner width

t- Liner thickness

As can be seen, the swelling force is directly related to the modulus of rupture, and therefore, the same amount that the swelling pressure is reduced by cation injection will reduce the induced modulus of rupture in the lining to the same extent.

However, the practical implementation of $Ca^{2+}$ injection in real-world projects must consider factors such as economic feasibility, environmental impact, and scaling challenges. While laboratory studies, such as the work by Han et al. [43] utilizing $CaCl_2$, have demonstrated advantages including low cost, non-toxicity, and minimal environmental contamination, these findings are established under controlled conditions. A critical transition must therefore be made from idealized laboratory settings to complex field environments. The potential influence of multi-ion chemistry, temperature fluctuations, and site-specific geochemical interactions on the treatment efficiency requires thorough investigation. Consequently, a detailed assessment of long-term performance, cost-effectiveness, and comprehensive environmental impact remains an essential focus for future field-scale research.

## 6. Conclusions

This research examined the swelling pressure of Marlstone in connection with cations, employing distilled water, $CaCl_2$ and NaCl, solutions at different concentrations for infiltration. The results demonstrate that the salinity of the infiltrating solutions has a considerable effect on the swelling pressure of Marlstone samples, with swelling pressure diminishing as the concentration of the infiltrating solutions increases. Moreover, at the same concentrations, the swelling pressure of Marlstone treated with $CaCl_2$ solutions was found to be lower than that of samples treated with NaCl solutions. Additionally, Marlstone saturated with $Ca^{2+}$ cations showed a higher resistance to leaching compared to those saturated with $Na^+$ cations. The findings of this research can be utilized to mitigate the detrimental effects of swelling behavior in structures situated in aquatic environments, such as hydropower plants constructed near marlstone formations. In these contexts, the potential for swelling can be reduced by injecting calcium wash-resistant ions, thereby preventing subsequent damage.

## 7. Limitations and Future Research Directions

- Given the limitations discussed, this research was restricted to two marlstone specimens. Future studies should expand the sample size to enhance the reliability of the results.
- A comprehensive evaluation of the economic feasibility and full environmental impact of $Ca^{2+}$ injection necessitates further investigation through full-scale field applications. The significant influence of real-world geochemical conditions, such as multi-ion interactions and temperature variations, also remains a critical area for future study.

## References

[1]. Tong, K., Pereira, J.M., Tong, K., Yu, F., Gue, J., Zihang, L., Dai, Z., & Chen, S. (2025). Microscopic swelling behaviors and structural responses of aggregate system: A coarse-grained molecular dynamics study. *Journal of Rock Mechanics and Geotechnical Engineering, 17*, 3833-3844.

[2]. Zhou, A., Du, J., Zaoui, A., Sekkal, W., & Sahimi, M. (2025). Molecular modeling of clay minerals: A thirty-year journey and future, *Coordination Chemistry Reviews, 526*, 216347.

[3]. Studds, P.G., Stewart, D.I., & Cousens, T.W. (1998). The effects of salt solutions on the properties of bentonite-sand mixtures. *Clay Minerals, 33*, 651-660.

[4]. Pusch, R. (2001). *Experimental Study of the Effect of High Porewater Salinity on the Physical Properties of a Natural Smectitic Clay*. Swedish Nuclear Fuel and Waste Management Co.

[5]. Mata, M.C. (2003). *Hydraulic Behaviour of Bentonite Based Mixtures in Engineered Barriers: The Backfill and Plug Test at the Äspö HRL (Sweden)*. University of Catalonia, 200 p.

[6]. Rao, M., & Shivananda, P. (2005). Role of osmotic suction in swelling of salt amended clays. *Canadian Geotechnical Journal, 42*, 307-315.

[7]. Suzuki, S., Prayongphan, S., Ichikawa, Y., & Chae, B. (2005). In situ observations of the swelling of bentonite aggregates in NaCl solution. *Applied Clay Science, 29*, 89-98.

[8]. Rao, S., Thyagaraj, T., & Thomas, H. (2006). Swelling of compacted clay under osmotic gradients. *Geotechnique, 56*, 707-713.

[9]. Rao, S.M., & Thyagaraj, T. (2007). Role of direction of salt migration on the swelling behaviour of compacted clays. *Applied Clay Science, 38*, 113-129.

[10]. Rao, S.M., & Thyagaraj, T. (2007). Swell-compression behaviour of compacted clays under chemical gradients. *Canadian Geotechnical Journal, 44*, 520-532.

[11]. Castellanos, E., Villar, M.V., Romero, E., Lioret, A., & Gens, A. (2008). Chemical impact on the hydro-mechanical behaviour of high-density FEBEX bentonite. *Physics and Chemistry of the Earth, Parts A/B/C, 33*, S516-S526.

[12]. Herbert, H.J., Kasbohm, J., Sprenger, H., Fernandez, A.M., & Reichelt, C. (2008). Swelling pressures of MX-80 bentonite in solutions of different ionic strength. *Physics and Chemistry of the Earth, Parts A/B/C, 33*, S327-S342.

[13]. Komine, H., Yasuhara, K., & Murakami, S. (2009). Swelling characteristics of bentonites in artificial seawater. *Canadian Geotechnical Journal, 46*, 177-189.

[14]. Siddiqua, S., Blatz, J., & Siemens, G. (2011). Evaluation of the impact of pore fluid chemistry on the hydromechanical behaviour of clay-based sealing materials. *Canadian Geotechnical Journal, 48*, 199-213.

[15]. Lee, J.O., Lim, J.G., Kang, I.M., & Kwon, S. (2012). Swelling pressures of compacted Ca-bentonite. *Engineering Geology, 129*, 20-26.

[16]. Ye, W., Zhang, Y., Chen, Y., Chen, B, & Cui, Y. (2013). Experimental investigation on the thermal volumetric behavior of highly compacted GMZ01 Bentonite. *Applied Clay Science, 83*, 210-216.

[17]. Siddiqua, S., Siemens, G., Blatz, J., Man, A., & Lim, B.F. (2014). Influence of pore fluid chemistry on the mechanical properties of clay-based materials. *Geotechnical and Geological Engineering, 32*, 1029-1042.

[18]. Ye, W.M., Zhang, F., Chen, B., Chen, Y.G., Wang, Q. & Cui, Y.J. (2014). Effects of salt solutions on the hydro-mechanical behavior of compacted GMZ01 Bentonite. *Environmental Earth Sciences, 72*, 2621-2630.

[19]. Wakim, J., Hadj-hassen, F. & De Windt, L. (2009). Effect of aqueous solution chemistry on the swelling and shrinkage of the Tournemire shale. *International Journal of Rock Mechanics and Mining Sciences, 46*, 1378-1382.

[20]. Zhu, C.M., Ye, W.M., Chen, Y.G., Chen, B., & Cui, Y.J. (2013). Influence of salt solutions on the swelling pressure and hydraulic conductivity of compacted GMZ01 bentonite. *Engineering Geology, 166*, 74-80.

[21]. Ye, W.M., Zhu, C.M., Chen, Y.G., Chen, B., Cui, Y.J., & Wang, J. (2015). Influence of salt solutions on the swelling behavior of the compacted GMZ01 bentonite. *Environmental Earth Sciences, 74*, 793-802.

[22]. Chen, Y.G., Zhu, C.M., Ye, W.M., Cui, Y.J., & Wang, Q. (2015). Swelling pressure and hydraulic conductivity of compacted GMZ01 bentonite under salinization–desalinization cycle conditions. *Applied Clay Science, 114*, 454-460.

[23]. Chen, Y.G., Zhu, C.M., Ye, W.M., Cui, Y.J., & Chen, B. (2016). Effects of solution concentration and vertical stress on the swelling behavior of compacted GMZ01 bentonite. *Applied Clay Science, 124*, 11-20.

[24]. Zhang, F., Ye, W.M., Chen, Y.G., Chen, B., & Cui, Y.J. (2016). Influences of salt solution concentration and vertical stress during saturation on the volume change behavior of compacted GMZ01 bentonite. *Engineering Geology, 207*, 48-55.

[25]. Liu, L.N., Chen, Y.G., Ye, W.M., Cui, Y.J., & Wu, D.B. (2018). Effects of hyperalkaline solutions on the swelling pressure of compacted Gaomiaozi (GMZ) bentonite from the viewpoint of $Na^+$ cations and $OH^-$ anions. *Applied Clay Science, 161*, 334-342.

[26]. Pejon, O.J., & Zuquette, L.V. (2002). Analysis of cyclic swelling of mudrocks. *Engineering Geology, 67*, 97-108.

[27]. Doostmohammadi, R., Moosavi, M., Mutschler, T., & Osan, C. (2007). *Swelling pressure of mudstone under cyclic wetting and drying*. In 11th Congress of the International Society for Rock Mechanics, Lisbon, 443-446.

[28]. Doostmohammadi, R., Moosavi, M., Mutschler, T., & Osan, C. (2009). Influence of cyclic wetting and drying on swelling behavior of mudstone in south west of Iran. *Environmental Geology, 58*, 999-1009.

[29]. Vergara, M.R., & Triantafyllidis, T. (2015). Swelling behavior of volcanic rocks under cyclic wetting and drying. *International Journal of Rock Mechanics and Mining Sciences, 80*, 231-240.

[30]. Komine, H. (2004). Simplified evaluation for swelling characteristics of bentonites. *Engineering Geology, 71*, 265-279.

[31]. Madsen, F.T., & Muller-Vonmoos, M. (1989). The swelling behaviour of clays. *Applied Clay Science, 4*, 143-156.

[32]. Savage, D. (2005). *The effects of high salinity groundwater on the performance of clay barriers*. Swedish Nuclear Power Inspectorate, Stockholm, 50 p.

[33]. Rao, S.M., Thyagaraj, T., & Rao, P.R. (2013). Crystalline and osmotic swelling of an expansive clay inundated with sodium chloride solutions. *Geotechnical and Geological Engineering, 31*, 1399-1404.

[34]. Wang, Q., Cui, Y.J., Tang, A.M., Delage, P., & Gatmiri, B. (2014). Long-term effect of water chemistry on the swelling pressure of a bentonite-based material. *Applied Clay Science, 87*, 157-162.

[35]. Bradbury, M.H., & Baeyens, B. (2003). Porewater chemistry in compacted re-saturated MX-80 bentonite. *Journal of Contaminant Hydrology, 61*, 329-338.

[36]. Villar, M.V. (2002). *Thermo-hydro-mechanical characterisation of a bentonite from Cabo de Gata, A study applied to the use of bentonite as sealing material in high-level radioactive waste repositories*. Publicación Técnica ENRESA, 210 p.

[37]. Kleijn, W.B., & Oster, J.D. (1982). A model of clay swelling and tectoid formation. *Clays and Clay Minerals, 30*, 383-390.

[38]. Bazali, T.L. (2022). Acritical investigation of diffuse double layer changes in clay-electrolyte systems at high tempratures. *Journal of Geophysics and Engineering, 19*, 940-954.

[39]. Tripathy, S., Sridharan, A., & Schanz, T. (2004). Swelling pressures of compacted bentonites from diffuse double layer theory. *Canadian Geotechnical Journal, 41*, 437-450.

[40]. Karnland, O. (1997). *Bentonite swelling pressure in strong NaCl solutions: correlation between model calculations and experimentally determined data*. Swedish Nuclear Fuel and Waste Management Co, 140 p.

[41]. Pusch, R., & Yong, R.N. (2006). *Microstructure of Smectite Clays and Engineering Performance*. Taylor & Francis, London and New York, 340 p.

[42]. Doostmohammadi, R., Moosavi, M., Mutschler, Th., & Osan, C. (2009). Influence of cyclic wetting and drying on swelling behavior of mudstone in south west of Iran. *Environmental Geology, 58*, 999-1009.

[43]. Han, S., Wang, B., Wang, Y., Liu, W., Chen, C., & Zhang, Y., (2024). Experimental study on soil improvement by electrochemical injection of calcium chloride solutions with time interval. *Scientific Reports, 14*, 15748.

انجمن مهندسی معدن ایران
نشریه مهندسی معدن و محیط زیست
نشانی نشریه: www.jme.shahroodut.ac.ir
دانشگاه صنعتی شاهرود

# بررسی فشار تورمی سنگهای مارنی در مجاورت کاتیون‌ها

امیررضا کاوندی و رامین دوست محمدی*

گروه مهندسی معدن، دانشکده مهندسی، دانشگاه زنجان، زنجان، ایران

**اطلاعات مقاله**

**تاریخ ارسال**: ۲۰۲۵/۰۱/۳۱

**تاریخ داوری**: ۲۰۲۵/۰۸/۲۸

**تاریخ پذیرش**: ۲۰۲۵/۰۹/۲۰

*DOI:10.22044/jme.2025.15669.3010*

**کلمات کلیدی**

کنترل تورم
قابلیت حفظ کاتیون
کاتیون $Ca^{2+}$
کاتیون $Na^{+}$

**چکیده**

تاکنون تحقیقات محدودی در مورد رفتار تورمی سنگ‌های مارنی در حضور کاتیون‌ها انجام شده است. در این مطالعه، آزمون‌های آزمایشگاهی با هدف تعیین فشار تورمی بر روی نمونه‌های سنگهای مارنی منطقه سد مراش در شمال غرب ایران، انجام شدند. نمونه‌ها پیش از نفوذ کاتیون‌ها، در معرض چرخه‌های تر و خشک شدن قرار گرفتند تا به شرایط تعادلی برسند. سپس نمونه‌ها با آب مقطر و با محلول‌های ۱، ۲ و ۳ مولار کلرید سدیم ($NaCl$) و کلرید کلسیم ($CaCl_2$) اشباع شدند. یافته‌ها حاکی از آن است که با افزایش غلظت محلول‌ها، فشار تورم سنگهای مارنی کاهش می‌یابد. علاوه بر این، در غلظت‌های یکسان، فشار تورم نمونه‌های اشباع‌شده با محلول‌های $CaCl_2$ کمتر از نمونه‌های تیمارشده با محلول‌های $NaCl$ بود. همچنین، سنگهای مارنی اشباع‌شده با یون‌های $Ca^{2+}$ در مقایسه با نمونه‌های اشباع‌شده با یون‌های $Na^{+}$، مقاومت بیشتری در برابر شستشو از خود نشان داد. یافته‌های این تحقیق می‌تواند برای کنترل فشار تورم سنگ‌های متورم شونده در مجاورت سیستم‌های نگهدارنده به کار گرفته شود.

نویسنده مسئول مکاتبات: ramin.doostmohammadi@znu.ac.ir (ر. دوست محمدی)